J. Austral. Math. Soc. Ser. B 26 (1984), 31–44

A NOTE ON THE INSTANTANEOUS STREAMLINES, PATHLINES AND PRESSURE CONTOURS FOR A CAVITATION BUBBLE NEAR A BOUNDARY

P. CERONE[1] and J. R. BLAKE[2]

(Received 27 April 1982; revised 24 December 1982)

Abstract

Instantaneous streamlines, particle pathlines and pressure contours for a cavitation bubble in the vicinity of a free surface and near a rigid boundary are obtained. During the collapse phase of a bubble near a free surface, the streamlines show the existence of a stagnation point between the bubble and the free surface which occurs at a different location from the point of maximum pressure. This phenomenon exists when the initial distance of the bubble is sufficiently close to the free surface for the bubble and free surface to move in opposite directions during collapse of the bubble. Pressure calculations during the collapse of a cavitation bubble near a rigid boundary show that the maximum pressure is substantially larger than the equivalent Rayleigh bubble of the same volume.

1. Introduction

One of the most likely causes of cavitation damage to turbomachinery blades is a high speed liquid jet that forms late in the collapse phase of a cavitation bubble. The jet can reach velocities of 130 to 180 ms^{-1} in water for realistic situations (Plesset and Chapman [13]). Rayleigh [15] examined the growth and collapse of a spherical cavity in an infinite fluid demonstrating the very large dynamic pressures arising during the collapse phase of the bubble life. Since Naudé and Ellis

[1]Department of Mathematics and Operations Research, Footscray Institute of Technology, P.O. Box 64, Footscray, Vic. 3011.
[2]Department of Mathematics, The University of Wollongong, P.O. Box 1144, Wollongong, N.S.W. 2500.

[9] showed that a bubble collapses asymmetrically when close to a boundary there have been a number of studies dedicated to the behaviour of a pulsating bubble near a boundary (Benjamin and Ellis [1], Gibson [5], Mitchell and Hammitt [11], Chahine [4], Gibson and Blake [6], [7] and Blake and Gibson [3]). The implications of these studies is that for a vapour cavity near a boundary the jet forms on the rearward side of a migrating bubble. For the two cases considered in this paper the jets move in differing directions during collapse of a bubble; away from a free surface and towards a rigid boundary.

Recently Chahine [4] examined the interaction between a collapsing bubble and a free surface showing that nonlinear theory should be used when the initial bubble centroid is within 2.2 maximum radii from the surface. Moreover, both Chahine [4] and Blake and Gibson [3] demonstrated the nonlinear interaction between the free surface and the cavity, showing that they move in opposite directions during the collapse phase when the centroid is approximately within one maximum radius. Clearly a stagnation point (that is, zero velocity) exists in such situations, although this point will move because it has an acceleration. Furthermore, the point of maximum pressure is generally not at the stagnation point. These two features are the product of the unsteady flow phenomena we are studying (in direct contrast to steady flow).

On the other hand an examination of bubble collapse near a rigid boundary reveals that much larger pressures develop in the vicinity of the jet on the opposite side of the bubble to the boundary. These pressures are found to be much larger than those near a similar sized Rayleigh bubble (see for example, Gibson [5]). Thus the rigid boundary intensifies the pressures surrounding a collapsing vapour bubble and these high pressures manifest themselves in the very high speed liquid jet.

The study of time dependent flows is one of the most rapidly developing areas in fluid mechanics due primarily to the advent of faster and larger computers together with improved algorithms for numerical techniques. Often our experience with steady flows is of little assistance in understanding unsteady flows as the flow fields are often totally different. For example in this paper, we obtain a stagnation point and a separate point of maximum pressure within the fluid (*i.e.*, not at the boundaries). In addition bubbles may deform and become multiply connected and hence admit circulation around the bubble. All of these features will be described in greater detail later in the paper.

In Section 2 we briefly describe the theory and the approximate integral equation technique suggested by Bevir and Fielding [2] and later used by Gibson and Blake [6]. Stagnation point flow is examined in Section 3 and the computations and results are discussed in Section 4.

2. Theory

We will assume the fluid is incompressible, inviscid and that surface tension and gravitational effects are negligible for most of the bubble lifetime (Plesset and Chapman [13], Blake and Gibson [3]). With these assumptions we may represent the velocity as the gradient of a potential which, in turn, satisfies Laplace's equation. That is

$$\mathbf{u} = \nabla\phi, \qquad \nabla^2\phi = 0, \tag{1}$$

where $\mathbf{u}$ is the Cartesian velocity vector and ϕ is the potential. The boundary conditions on the fluid at infinity are

$$\mathbf{u} \to \mathbf{0} \quad \text{and} \quad p \to p_\infty, \tag{2}$$

where p is the pressure and p_∞ is the constant pressure at infinity and on the free surface. On the cavity surface we have

$$\mathbf{u}_s = \mathbf{u}, \qquad p = p_c, \tag{3}$$

where $\mathbf{u}_s$ is the velocity of a particle on the surface and p_c is the saturated vapour pressure in the cavity and which is assumed constant. Applying the dynamic boundary condition on the cavitation bubble surface yields,

$$p_c = p_\infty - \rho\frac{\partial\phi}{\partial t} - \frac{1}{2}\rho|\mathbf{u}|^2, \tag{4}$$

where ρ is the density of the fluid.

For the rigid boundary case there is no flow across the boundary, thus,

$$\frac{\partial\phi}{\partial x} = 0 \quad \text{at } x = 0. \tag{5}$$

For the nonlinear free surface problem we equate the Bernoulli pressure to that on the free surface (that is, p_∞) to obtain

$$\frac{\partial\phi}{\partial t} + \frac{1}{2}|\mathbf{u}|^2 = 0 \quad \text{on } x = \xi(r, t), \tag{6}$$

where $\xi(r, t)$ is the displacement of the free surface.

The growth and collapse phases of a cavitation bubble are modelled using a combined Lagrangian-Eulerian description of the bubble and fluid motion: a Lagrangian approach to describe the bubble surface and an Eulerian representation of the flow field.

To initiate the calculations, we suppose that the cavitation bubble is very small with a radius R_0 which is very much less than the distance to the boundary. This approximation allows us to use the potential for a spherical cavity in an infinite

https://doi.org/10.1017/S0334270000004318 Published online by Cambridge University Press

fluid as our initial condition on the bubble surface, namely

$$\phi_0 = -R_0\left\{\frac{2}{3}\left(\frac{p_\infty - p_c}{\rho}\right)\left[\left(\frac{R_m}{R_0}\right)^3 - 1\right]\right\}^{1/2}, \tag{7}$$

where R_m is the maximum bubble radius which is determined by p_∞, p_c and the initial kinetic energy given to the fluid. In the free surface example, we also need to specify the initial potential on the free surface: linear theory is adequate for this stage which shows us that $\phi_0 = 0$ on $\xi = 0$.

We obtain the solution using an approximate integral equation approach similar to that suggested by Bevir and Fielding [2]. The potential is specified in terms of a Fredholm integral equation of the first kind and a distribution of singularities along the axis of symmetry completely contained within the bubble is used to solve the problem. Although there are obvious difficulties with uniqueness using this approach, in that we can only hope to approximate the solution in a least squares sense, we will use it because of its simplicity and accurate prediction (Gibson and Blake [6]) of features observed experimentally. We refer the reader to Blake and Gibson [3] for a detailed description of the numerical technique (although they used ring distributions as against the simpler line distribution used in this paper). Conservation of mass, momentum and energy is examined at each time step to ensure that variation is within specified bounds.

It is advantageous to specify the problem in terms of dimensionless variables. Following Gibson and Blake [6] linear dimensions are nondimensionalised with respect to the maximum bubble size R_m as follows (capitals imply the dimensionless variable, except for γ which specifies the initial location of the bubble),

$$X = x/R_m, \qquad R = r/R_m, \qquad \gamma = h/R_m. \tag{8a}$$

The characteristic collapse velocity $[(p_\infty - p_c)/\rho]^{1/2}$ enables us to define a time scale t^* and hence dimensionless time T by

$$T = t/t^*, \qquad t^* = \left(\frac{\rho R_m^2}{p_\infty - p_c}\right)^{1/2}. \tag{8b}$$

Pressure is conveniently made dimensionless by

$$P = \frac{p - p_c}{p_\infty - p_c}, \tag{8c}$$

yielding $P = 0$ on the bubble and $P = 1$ at infinity (and on the free surface). The potential ϕ is made dimensionless with respect to $R_m[(p_\infty - p_c)/\rho]^{1/2}$. The Stokes stream function may be obtained from the potential in cylindrical polar

coordinates *via* the following relation,

$$\frac{\partial \phi}{\partial x} = \frac{1}{r}\frac{\partial \psi}{\partial r}, \qquad \frac{\partial \phi}{\partial r} = -\frac{1}{r}\frac{\partial \psi}{\partial x}. \tag{9}$$

In obtaining the updated value for the potential on the free surfaces Blake and Gibson [3] were able to eliminate the $\partial\phi/\partial t$ term by using the dynamic boundary conditions (4) and (6). However, this is not possible when calculating the pressure through the Bernoulli condition

$$p = p_\infty - \rho\frac{\partial \phi}{\partial t} - \frac{1}{2}\rho|\mathbf{u}|^2, \tag{10}$$

at any general point, in the fluid. In our calculations we use a backward difference approximation,

$$\frac{\partial \phi^n}{\partial t} \approx \frac{\phi^n - \phi^{n-1}}{\Delta t}.$$

ϕ and $|\mathbf{u}|$ may be evaluated at any point (x_j, r_j) since at each time step the source strength has been calculated.

The procedure for the rigid boundary case is similar to that outlined above except that marked particles need only be taken on the cavity surface as the solution method automatically satisfies the boundary condition (5).

To determine the instantaneous streamlines and pressure contours for both the nonlinear free surface and the rigid boundary problems, their numerical values are obtained at specified equispaced grid points of the (x, r) plane. A contouring procedure is used after having determined the minimum and maximum values in the fluid. The results will be discussed subsequently, however we first consider flow about a stagnation point in unsteady flow.

3. Stagnation point flow

For sufficiently small γ ($\gamma \leqslant 1.1$) in the free surface example, an instantaneous stagnation point appears in the fluid on the axis of symmetry between the two free surfaces. Thus, following Longuet-Higgins [9] we may expand the stream function about the stagnation point $x_0(t)$ to produce,

$$\psi = \psi_0(t) + \tfrac{1}{2}\alpha(t)(x - x_0)r^2 + 0(x^2r^2, xr^3). \tag{11}$$

The equivalent expression for ϕ is,

$$\phi = \phi_0(t) + \tfrac{1}{2}\alpha(t)(x - x_0)^2 + 0(x^3, x^2r). \tag{12}$$

https://doi.org/10.1017/S0334270000004318 Published online by Cambridge University Press

We are now in a position to show that the point of maximum pressure does not correspond to the stagnation point as it would in steady flow. From the Bernoulli pressure condition (10) and using (12) it may easily be shown that the pressure may be approximated by

$$\left.\begin{aligned} p &\approx p_0(t) + \rho\kappa_1(x - x_0) - \tfrac{1}{2}\rho\kappa_2(x - x_0)^2 \\ \text{where } p_0(t) &= p_\infty - \rho\phi_0(t),\ \kappa_1 = x_0'\alpha \text{ and } \kappa_2 = \alpha' + \alpha^2. \end{aligned}\right\} \tag{13}$$

Hence, it may be shown from (13) that, for $\kappa_2 > 0$, the maximum pressure occurs at

$$x = x_0 + \kappa_1/\kappa_2$$

with a value

$$p_{\max} = p_0(t) + \tfrac{1}{2}\rho\kappa_1^2/\kappa_2. \tag{14}$$

Thus the point of maximum pressure occurs at a different location from the stagnation point provided $\kappa_1 \neq 0$.

4. Computations and discussion

A. Preliminaries: the Rayleigh bubble

The Rayleigh bubble solution for a spherical bubble in an infinite fluid invokes spherical symmetry. Mass conservation implies that the velocity field can be represented by a time-dependent mass source at the origin. Clearly the instantaneous streamlines are radial. Furthermore the dynamic boundary condition enables us to obtain an algebraic expression for the dimensionless pressure as a function of only the bubble radius R^* and the radial coordinate r^*, as follows,

$$P(r) = 1 + \frac{1}{r^*}\left(\frac{1 - 4R^{*3}}{3R^{*2}}\right) - \frac{R^*(1 - R^{*3})}{3r^{*4}}. \tag{15}$$

The maximum pressure occurs at $r^* = r_1^*$, where

$$r_1^* = \begin{cases} R^*\left(\dfrac{4(1 - R^{*3})}{1 - 4R^{*3}}\right)^{1/3}, & R^* \leqslant 0.6299; \\ \infty, & R^* \geqslant 0.6299. \end{cases} \tag{16}$$

For example with $R^* = 0.1$, $r_1^* = 0.157$ and $P_{\max} = 157.7$. Thus, in the forthcoming discussion in this section, we will be highlighting the similarities and variations from the Rayleigh bubble solution.

https://doi.org/10.1017/S0334270000004318 Published online by Cambridge University Press

B. Flow description of a bubble near a free surface

(i) *Streamlines*

The instantaneous streamlines were calculated for the growth and collapse phases of a vapour cavity near a free surface. Using the approximate integral equation technique described in Blake and Gibson [3], a small bubble of dimensionless radius 0.1, initially located at one maximum radius from the free surface was allowed to grow and collapse.

The bubble grows spherically for about a third of its life time migrating slowly towards the 'flat' free surface. For $\gamma \leqslant 1.1$ the top half of the vapour bubble becomes elongated and is entrained within the raised free surface compared to the more hemispherical bottom half. During the collapse phase the vapour bubble migrates away from the free surface while, at the same time, the free surface continues to expand. This nonlinear interaction between the free surface and the bubble leads to the formation of two opposing jets which produce a stagnation point on the axis of symmetry between the surfaces.

Figure 1 shows the stagnation point and instantaneous equispaced streamlines for dimensionless time $T = 0.797$, 0.897, 0.993 and 1.120. Of particular interest is the high density of streamlines joining the 'shortest distance' between the two uppermost free surfaces. This and other aspects of nonlinear interaction between the free surfaces will be discussed at greater length when we consider the pressure contours.

In a recent theoretical and experimental study on the growth and collapse of a cavitation bubble near a free surface Chahine [4] shows that nonlinear theory should be used when the bubble centroid depth h is less than 2.2 of the maximum radius (*i.e.*, $\gamma < 2.2$). Chahine [4] and Blake and Gibson [3] (see also Van Dyke [16]) observed that for cases when the bubble centroid depth is approximately equal to R_m, the free surface and the bubble move in opposite directions during the collapse phase.

When the bubble was initially located at $\gamma = 1.5$ no stagnation point was formed and the free surface grew and collapsed with the growth and collapse of the vapour cavity. Theory would suggest that the changeover point for the formation of opposing jets is around $\gamma = 1.1$.

(ii) *Pathlines*

The Lagrangian description of both the free surface and the vapour cavity enables us to trace the path of the "marked particles" on both surfaces. Figure 2 shows the pathlines of some of these particles together with the shape of both

https://doi.org/10.1017/S0334270000004318 Published online by Cambridge University Press

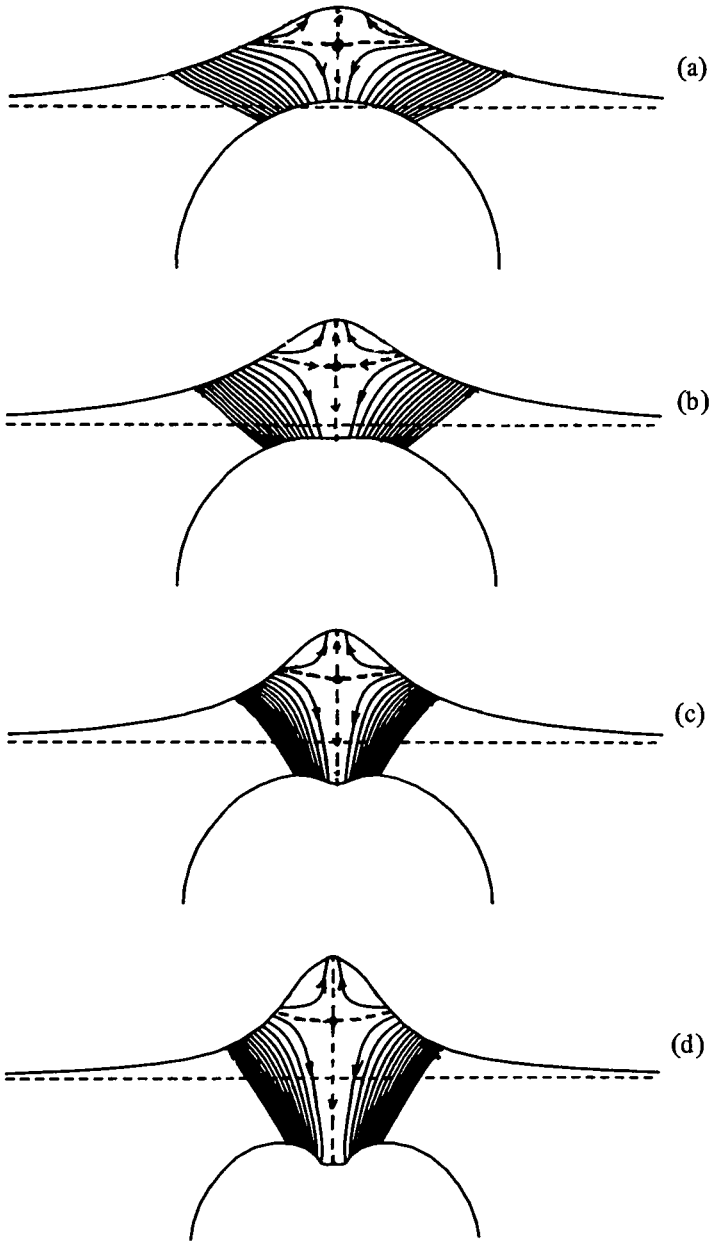

Figure 1. Instantaneous streamlines during the collapse of a vapour cavity initially one maximum bubble radius from a free surface for dimensionless time (a): 0.797, (b): 0.897, (c): 0.993 and (d): 1.12. A stagnation point exists on the axis of symmetry during the collapse phase of the bubble. The approximate lifetime of the bubble in this example is $T = 1.4$.

https://doi.org/10.1017/S0334270000004318 Published online by Cambridge University Press

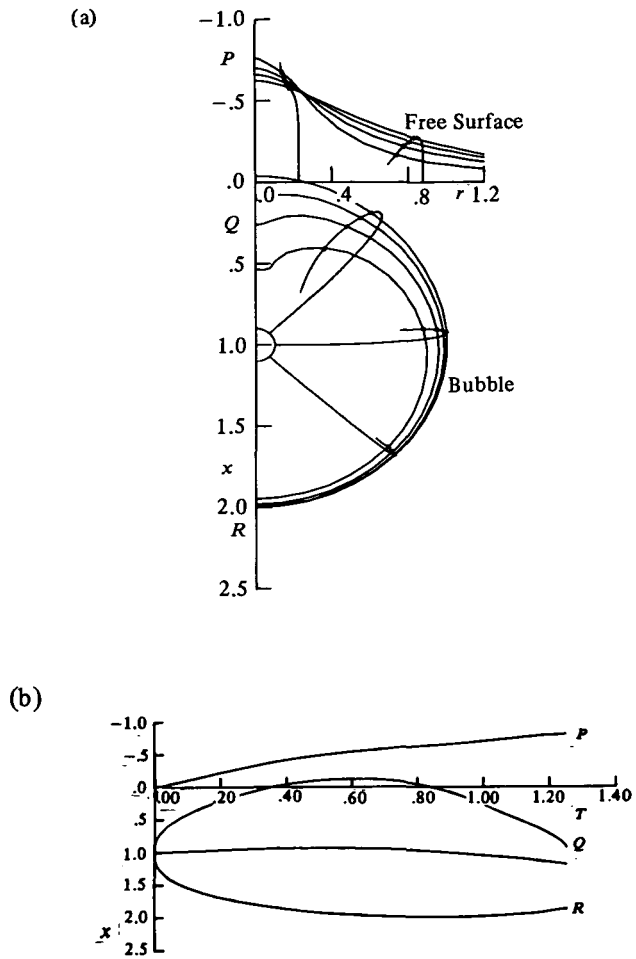

Figure 2. (a) Trajectories (.) of fluid particles on the surface of the vapour cavity and on the free surface. The bubbles shown are at the same time as in Figure 1, together with the initial cavity of radius 0.1. (b) Movement of particles on the axis of symmetry corresponding to P, Q and R in (a) with time.

surfaces. We may notice from the figure that the particles move radially during the growth phase similar to the Rayleigh bubble. However, as the bubble begins to collapse, the particles migrate towards the axis of symmetry while the jet and free surface spikes continue to grow in opposite directions resulting in the formation of a stagnation point on the axis.

https://doi.org/10.1017/S0334270000004318 Published online by Cambridge University Press

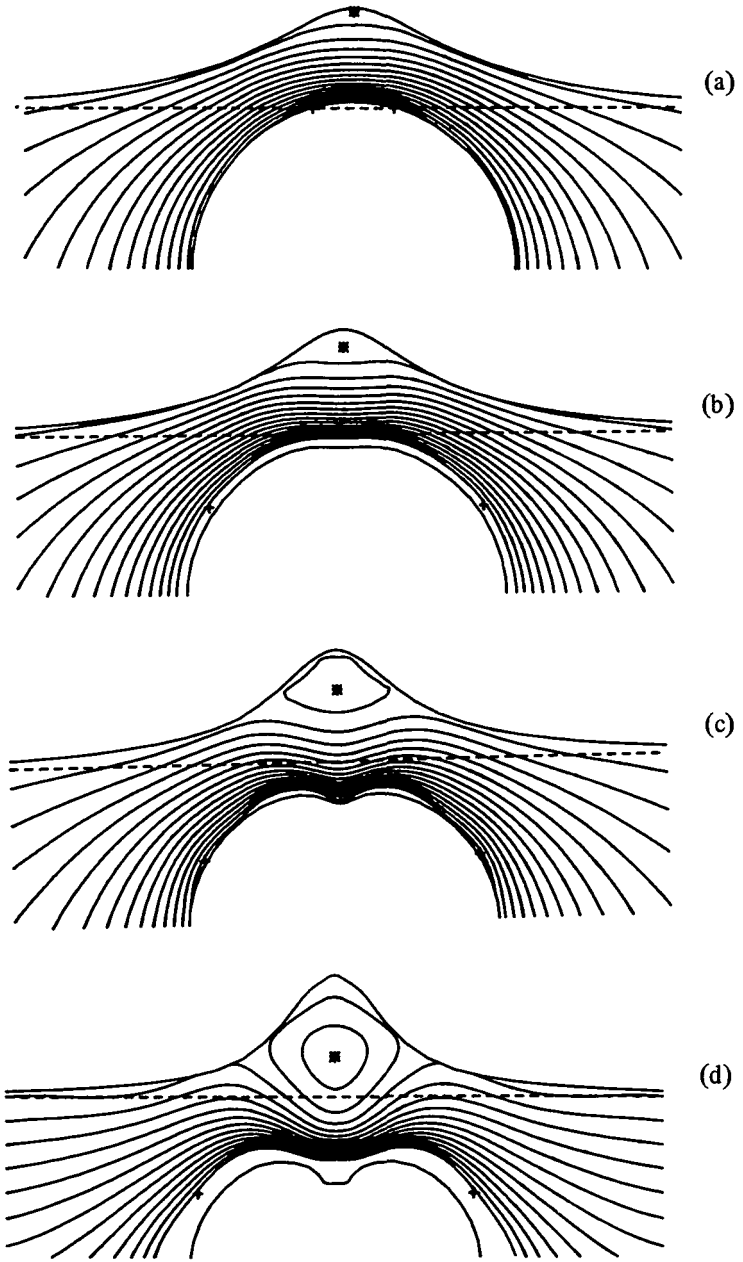

Figure 3. Equally spaced pressure contours for a vapour bubble near a free surface initially located at one maximum bubble radius from the free surface. The times for (a), (b), (c) and (d) correspond to Figure 1. A point of maximum pressure occurs on the axis between the bubble and free surface (*).

https://doi.org/10.1017/S0334270000004318 Published online by Cambridge University Press

(iii) *Pressure*

In Figure 3, equispaced pressure contours are shown for the case of $\gamma = 1.0$. The dimensionless times in the four examples illustrated in Figure 3 correspond exactly to those in Figure 1. It is clear on comparing Figures 1 and 3 that the stagnation point and the point of maximum pressure do not generally coincide, as was anticipated in Section 3. In a recent paper Longuet-Higgins [10] analysed Figure 10 in Blake and Gibson's [3] paper and has suggested that in the free surface spike the constant pressure contours, which includes the free surface, correspond to a Dirichlet hyperboloid. Although our contours are produced by a contouring package and may not be accurate in regions of high curvature, there is some suggestion that the contours are hyperboloidal.

Physically during the bubble collapse phase fluid is drawn in towards the bubble from the region of least impedance, or more correctly, inertance. In practical terms this corresponds to the shortest distance, and hence least mass, between the two uppermost free surfaces. As the fluid is drawn in, a point of maximum pressure is created on the axis of symmetry forcing the fluid to move in opposing directions and hence creating an instantaneous stagnation point.

C. Flow description of a bubble near a rigid boundary

(i) *Streamlines*

Streamlines were obtained for a vapour cavity growing and collapsing near a rigid boundary which was initially located at $\gamma = 1.0$. In the growth phase the bubble is almost spherical with a slight flattening, as one might expect, near the rigid boundary. This impedance of motion near the boundary results in a slight migration of the bubble centroid away from the boundary during the growth phase. However during the collapse phase the bubble centroid migrates towards the boundary because of the high impedance of the boundary. A translating collapsing bubble is unstable (*e.g.*, Plesset and Mitchell [14]), the dominant instability being realised in a jet which threads the collapsing bubble from the rear.

Figure 4(a) illustrates the instantaneous streamlines soon after the formation of the jet. Ultimately the jet will penetrate the free surface of the bubble on the other side to form a multiply connected region. The flow field at this stage would correspond to a ring vortex to preserve the impulse generated throughout the life time of the bubble (see *e.g.*, Benjamin and Ellis [1], Lauterborn [8]). In Figure 4(a) we can see the initial stages of the development of a ring vortex by the

https://doi.org/10.1017/S0334270000004318 Published online by Cambridge University Press

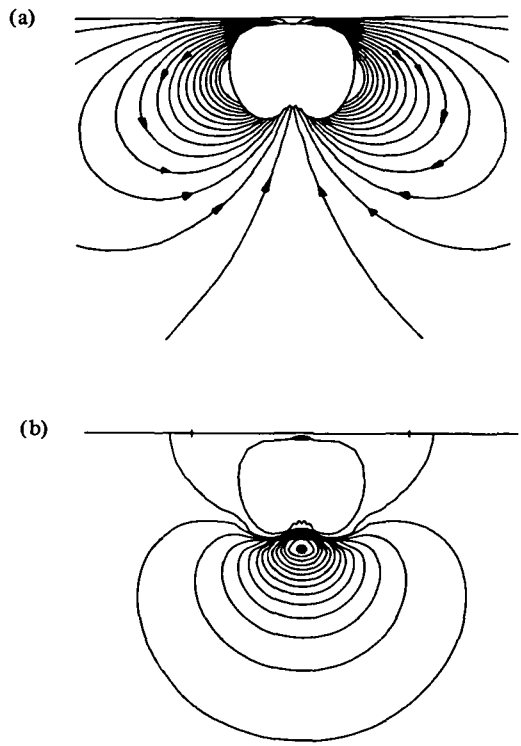

Figure 4. Cavitation bubble near a rigid boundary for $\gamma = 1.0$ and time $= 2.06$. (a) Instantaneous streamlines. (b) Pressure contours with maximum at * of 6.66.

collapsing bubble. Previous models of Plesset and Chapman [13] and Bevir and Fielding [2] which only simulated the collapse phase of an initially spherical cavity, obtain bubble shapes which are much more elongated than those obtained here.

(ii) *Pressure*

During the growth phase the pressure contours are essentially the same as for the Rayleigh bubble being approximately spherical. However, the major change occurs during collapse when the spherical symmetry is completely lost. A point of high pressure forms on the opposite side of the cavity from the rigid boundary before there is any sign of a jet being formed. The pressures increase extremely fast as the jet is formed (see Figure 4(b)). It is this high pressure build up and the subsequent high jet velocities which are thought to be one of the principal mechanisms for cavitation damage. Table 1 shows the effect of a rigid boundary

https://doi.org/10.1017/S0334270000004318 Published online by Cambridge University Press

on the pressure produced near a vapour cavity. The maximum pressure obtained within a 4×3 maximum radii region is compared with pressures at the same distance for a spherical cavity of equal volume in an infinite fluid. The pressures are close until the jet starts to form at which stage the pressure is much greater for the rigid boundary case. Gibson [5] shows that extremely high pressures exist close to a small Rayleigh bubble. However for a cavity with radii greater than 0.66 the maximum pressure is ambient (that is, p_∞). Thus the ambient pressure is approached the further away we are from the bubble and would yield the maximum value of $P = 1$ if we were to extend the grid to infinity. It is for this reason that the maximum pressures shown in Table 1 occur at the extremities except for the last two times at which stage the jet has begun to form.

TABLE 1. Maximum pressure in a 4×3 grid for a vapour cavity near a rigid boundary compared with that of an equivalent size Rayleigh bubble. The cavity is initially one maximum bubble radius from the rigid boundary ($\gamma = 1.0$).

Time	Centroid	Equivalent Radius	Distance	Maximum Pressure	
				Rayleigh	Rigid Boundary
0.22	1.0283	0.6866	2.8085	0.7795	0.8228
0.62	1.0543	0.9382	2.7903	0.6588	0.6350
1.02	1.0363	1.0106	2.8029	0.6405	0.5891
1.42	0.9613	0.9684	2.8560	0.6580	0.6339
1.82	0.7695	0.7926	2.9958	0.7337	0.8301
2.02	0.5492	0.6154	0.7508	0.8916	3.7342
2.06	0.4806	0.5621	0.6194	1.5977	6.6606

5. Conclusion

Our description of the flow field about a collapsing vapour cavity near a rigid boundary and a free surface has supplemented and extended the available knowledge on the mechanisms involved. This work has demonstrated that the spectacular movement of the free surface in the opposite direction to the jet developed in the vapour cavity gives rise to a stagnation in the flow field which is at a different location from the point of maximum pressure. The effect of a rigid boundary in producing extremely high pressures which cause the formation of the subsequent liquid jet, are shown to be larger than the pressures involved for a bubble in an infinite fluid, possibly causing pressure initiated damage to the boundaries in addition to the damage mechanism due to the impact of the jet.

https://doi.org/10.1017/S0334270000004318 Published online by Cambridge University Press

References

[1] T. B. Benjamin and A. T. Ellis, "The collapse of cavitation bubbles and the pressure thereby produced against solid boundaries", *Phil. Trans. Roy. Soc. London Ser. A* 260 (1966), 221–240.

[2] M. K. Bevir and P. J. Fielding, "Numerical solution of incompressible bubble collapse with jetting", in *Moving boundary problems in heat flow and diffusion* (eds. J. R. Ockendon and W. R. Hodgkins), (Clarendon Press, Oxford, 1975), 286–294.

[3] J. R. Blake and D. C. Gibson, "Growth and collapse of a vapour cavity near a free surface", *J. Fluid Mech.* 111 (1981), 123–140.

[4] G. L. Chahine, "Interaction between an oscillating bubble and a free surface", *Trans. ASME Ser. I J. Fluids Engng.* 99 (1979), 709–716.

[5] D. C. Gibson, "Cavitation adjacent to plane boundaries", *Proc. 3rd Austral. Hydraulics and Fluid Mech. Conf., Sydney* (The Institution of Engineers, Australia, 1968), 210–214.

[6] D. C. Gibson and J. R. Blake, "Growth and collapse of cavitation bubbles near flexible boundaries", *Proc. 7th Austral. Hydraulics and Fluid Mech. Conf.* (1980), 283–286.

[7] D. C. Gibson and J. R. Blake, "The growth and collapse of bubbles near deformable surfaces", *Appl. Sci. Res.* 38 (1982), 215–224.

[8] W. Lauterborn, "Cavitation bubble dynamics—new tools for an intricate problem", in *Mechanics and physics of bubbles in liquids*, (cd. L. van Wijngaarden), (Nijhoff, The Hague, 1982), 165–178.

[9] M. S. Longuet-Higgins, "A technique for time-dependent free-surface flows", *Proc. Roy. Soc. London Ser. A* 371 (1980), 441–451.

[10] M. S. Longuet-Higgins, "Bubbles, breaking waves and hyperbolic jets at a free surface", *J. Fluid Mech.* 127 (1983), 103–122.

[11] T. M. Mitchell and F. G. Hammitt, "Asymmetric cavitation bubble collapse", *Trans. ASME Ser. I J. Fluids Engng.* 95 (1973), 29–37.

[12] C. F. Naudé and A. T. Ellis, "On the mechanism of cavitation damage by non-hemispherical cavities collapsing in contact with a solid boundary", *Trans. ASME Ser. D J. Basic Engng.* 83 (1961), 648–656.

[13] M. S. Plesset and R. B. Chapman, "Collapse of an initially spherical vapour cavity in the neighbourhood of a solid boundary", *J. Fluid Mech.* 47 (1971), 283–290.

[14] M. S. Plesset and T. P. Mitchell, "On the stability of the spherical shape of a vapour cavity in a liquid", *Quart. Appl. Math.* 13 (1956), 419–430.

[15] Lord Rayleigh, "On the pressure developed in a liquid during the collapse of a spherical void", *Phil. Mag.* 34 (1917), 94–98.

[16] M. Van Dyke, *An album of fluid mechanics* (Parabolic, Stanford, 1982), 108.